中國機械工程學刊第三十九卷第五期第 471~476 頁(民國一百零七年)
Journal of the Chinese Society of Mechanical Engineers, Vol.39, No.5, pp 471~476 (2018)

A Multi Degree of Freedom Motion Platform with Micro-pusher using Additive Manufacture Technology

Yi-Cheng Chen[*,**] and Sheng-Chih Shen[*]

Keywords： Additive Manufacturing; MDOF motion platform; Micro-pusher; Piezoelectric actuator.

ABSTRACT

A novel multi-degree-of-freedom (MDOF) motion platform was developed using symmetric piezoelectric plate and a Ni alloy micro-pusher element. An additive manufacturing (AM) technique was employed to manufacture a Ni alloy micro-pusher, which was then attached at the midpoint of the long side of a piezoelectric plate with dual electrodes to construct a symmetric piezoelectric actuator (SPA). The research integrated the concept of bricks, and three different vibration modes of the SPA were designed to develop a MDOF motion platform, which was able to rotate a hemisphere *device* along three perpendicular axes. The experiment demonstrated the MDOF motion platform working frequencies along the X, Y, and Z axes to be 223.6, 223.2, and 225 kHz and the rotation speeds to reach 76 rpm, 71 rpm, and 192 rpm, respectively, at a driving voltage of $30V_{pp}$. In the future, this MDOF motion platform may be used for a number of applications, such as portable mobile devices and sun-tracking systems in green energy harvesters.

INTRODUCTION

Portable mobile devices have become increasingly popular in recent years, and the consumption of portable batteries has also increased environmental pollution. As a result, people are exploring alternative energy sources to reduce pollution. Although commercial portable solar chargers are convenient, the energy they collect is still insufficient because of the lack of sun tracking capability. In addition, robots are being miniaturized with the aim of generating human-like motion, and it is therefore necessary to develop microactuators that can generate dexterous, precise motions, such as multi-degree-of-freedom (MDOF) microactuators. The study will focus on the design of multi degree of freedom (MDOF) motion platform which can be used as the direct drive motor for joints of industrial robotic arm or other portable compact device. Compare to traditional motor system, a piezoelectric based motion platform can reduce the volume therefore scale down the driving chain. Electromagnetic and piezoelectric actuators are the two types of microactuators that are presently widely available in commerce. Electromagnetic actuators are constructed using components such as magnetic materials, coils, gears, and screws, which induce magnetic force to move the rotor, achieving multi-degree motion; however, the magnetic field strength is limited by the size of the microactuator, and when the components are reduced in size, the energy output is also reduced. The magnetic actuators have low efficiency in the power range lower than 30W (K. Uchino, 2008). Therefore, an electromagnetic actuator is unfavorable to miniaturization for a high-power microactuator. Piezoelectric actuators are designed using a different vibration mode and can easily achieve multi-degree motion, and hence these actuators have a relatively simple structure and are much smaller in terms of volume and weight than electromagnetic actuators. In other words, the piezoelectric actuator employs a frictional force to drive the rotor. According to the scaling law, when the scale decreases, the electromagnetic force decreases more rapidly than the friction force (S. Baglio et al. 2008); therefore, piezoelectric actuators are suitable for applications requiring miniaturization.

From 2001 onward, Takemura et al. (2004) developed a MDOF piezoelectric microactuator with a compact plate stator and a spherical rotor that used pusher-shaped vibrators with a dual-phase mode. Otokawa (2004) proposed a MDOF piezoelectric microactuator consisting of four pusher-shaped vibrators with a single-phase mode. Single-phase mode MDOF microactuators with pusher-shaped vibrators commonly use a resonant frequency to create

Paper Received May, 2018. Revised October, 2018. Accepted October, 2018. Author for Correspondence: Yi-Cheng Chen

**Department of Systems and Naval Mechatronic Engineering, National Cheng Kung University, Tainan, Taiwan 701, ROC.*

***Intelligent Mechatronics Department, Smart Micro-systems Technology Center, Industrial Technology Research Institute*

independent vibration modes in each piezoelectric plate, thus allowing the rotor to rotate on three perpendicular axes. Therefore, MDOF microactuators driven by a single phase are simpler and easier to downsize than dual-phase microactuators (O. Vyshnevskyy et al., 2005). A single-phase mode actuator was developed by switching different single-phase modes for each vibrator to promote rotor movement (K. Otokawa et al., 2007), whereas dual-phase mode actuators must be simultaneously excited by the longitudinal vibration mode and the bending vibration mode to create a motion trajectory (Nanomotion LTD., 1995 & S. T. HO, 2006). The driver circuit of the dual-phase mode actuators requires at least two groups of driving signals to achieve synchronization resonance, but it is difficult to control the two frequencies precisely that must correspond with each other completely. A feature of single-phase mold MDOF actuators with pusher-shaped vibrators is the use of resonant frequency to create independent vibration modes in each piezoelectric plate, thus allowing the rotor to rotate on three perpendicular axes. Therefore, MDOF microactuator driven by a single phase are easier to downsize and have simpler form than those driven by dual phases, and thus in this design a small stator is able to drive a large ball rotor. Therefore, this study proposes a novel piezoelectric microactuator with pusher-shaped vibrators, which only requires the combination of three vibrators driven by a single phase to move a hemisphere device along three perpendicular axes.

DESIGN AND FABRICATION

A driving voltage was applied on a square piezoelectric plate with a piezoelectric strain constant of d31, generating an extension/contraction movement at the edges of the plate. A symmetric piezoelectric actuator (SPA) was then designed using two square piezoelectric plates to form a rectangular piezoelectric plate based on this extension/contraction movement. The Lead Zirconate-Titanate (PZT) with Perovskite structure is used as the material of the proposed piezoelectric actuator because of its superior performance in electro-mechanical transformation characteristic. The SPA polarization was along the thickness dimension (Z direction), which generated the d31 piezoelectric strain constant as shown in Fig.1. Two symmetric square electrodes A and B were then placed on the front side of the large surface (X–Y plane). Each electrode covered one-half of the surface, whereas the rear surface had a single electrode that served as a common drain. The micro-pusher was attached at the midpoint P of one long edge of the piezoelectric plate. Movement of the midpoint P in different directions was achieved by switching the applied voltage between the symmetric electrodes.

The micro-pusher was fabricated layer by layer by combining the maskless lithography system and additive manufacturing (AM) technology. Fabricating the micro-pusher by AM technology can rough the surface and enhance the thrust. The study utilized the Ni-Alloy powder as the material to sinter the micro-pusher. First, spread the Ni-Alloy powder on a platform and flat it by a scraper. Second, sinter the powder with a specific shape then low down the platform. Repeat the first and the second steps till the micro-pusher is completed. The fabrication parameters of the micro-pusher is shown below: Laser power: 28 W, Sintering speed: 8 mm/s, Laser frequency: 140 Hz. With the above parameters, the optimum porosity (4.67%) of sintered Ni-Alloy power was obtained. The length, width, and thickness of the micro-pusher were 1.5 mm, 3 mm, and 0.5 mm, respectively. The micro-pusher was mounted at midpoint P of the SPPE X–Z plane to enhance its driving capability. This novel SPPE structure completely avoids the abrasion problem of ceramic micro-pushers by adopting a Ni alloy micro-pusher.

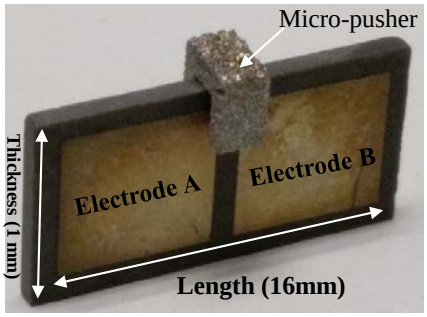

Fig. 1 Structure of symmetric piezoelectric actuator (SPA).

Dynamic analysis of the SPPE

The SPPE is excited by placing a signal on one of the electrodes on the front side. The other front electrode is left floating. The excitation signal is the resonant frequency of a vibration mode of the SPPE. This mode is that of a two-dimensional standing wave. It can be thought of as the superposition of standing waves in two directions. When a driving voltage is applied on a SPPE and movement of the micro-pusher can be generated in different directions. Therefore, the displacement of micro-pusher (i.e. midpoint P) can be expressed as

$$\begin{cases} u_x = A_x \cos\lambda y \cos\xi x \cos\varpi t \\ u_y = A_y \sin\lambda y \cos\xi x \cos\varpi t \\ u_z = 0 \end{cases} \quad (1)$$

where u is the displacement, A is the amplitude, and λ and ξ are the wave numbers. As the SPPE has a standing wave driving component, the displacement of micro-pusher can be expressed as in Eq (1). As SPPE surface can be divided into A and B with two symmetrical electrodes, when the driving voltage is applied on A or B electrodes then the displacement of

micro-pusher from each electrode can therefore be expressed as in Eqs (2) and (3), respectively

$$\begin{cases} u_{xA} = A_x \cos\lambda y \cos\xi x \cos\varpi t \\ u_{yA} = A_y \sin\lambda y \cos\xi x \cos\varpi t \end{cases} \quad (2)$$

$$\begin{cases} u_{xB} = -A_x \cos\lambda y \cos\xi x \cos(\varpi t + \varphi) \\ u_{yB} = A_y \sin\lambda y \cos\xi x \cos(\varpi t + \varphi) \end{cases} \quad (3)$$

where u_{xA} and u_{xB} represent the displacement in the X direction of the A and B electrodes, respectively, and u_{yA} and u_{yB} represent the displacement in the Y direction of the A and B electrodes, respectively. The resultant movement of micro-pusher on X-Y plane can be calculated by Eqs (2) and (3).

$$\left(\frac{u_x}{-2A_x \cos\lambda y \cos\xi x \sin\frac{\varphi}{2}}\right)^2 + \left(\frac{u_y}{2A_y \sin\lambda y \cos\xi x \cos\frac{\varphi}{2}}\right)^2 = 1 \quad (4)$$

From Eq (4), it can be seen that when φ=0 or φ=π, micro-pusher has a straight-line trajectory along the Y direction or X direction and when φ≠0 or φ≠π, micro-pusher has an elliptical trajectory. As a result, the micro-pusher amplitude along a line inclined with respect to the plate surface. Therefore, based on the equations above, the three vibration modes of the SPPE can be obtained, when both electrodes A and B are excited with signal-phase mold at the same time, this is defined as mode (1, 1) and φ=0. therefore, the Eq (4) can be expressed as this indicates that micro-pusher has no displacement in the X direction and a straight-line trajectory in the Y direction.

$$\begin{cases} u_x = 0 \\ u_y = 2A_y \sin\lambda y \cos\xi x \end{cases} \quad (5)$$

When only electrode A is excited, this is defined as mode (1,0). The movement of micro-pusher can be obtained from Eq (2), and shows that micro-pusher will move in the direction of the inclination at Quadrant I, i.e.:

$$u_{xA} = \frac{A_x}{A_y}\frac{\cos\lambda y}{\sin\lambda y} u_{yA} \quad (6)$$

When only electrode B is excited, this is defined as mode (0,1). The movement of micro-pusher can be obtained from Eq (3), and shows that micro-pusher will move in the direction of the inclination at Quadrant II, i.e.:

$$u_{xB} = -\frac{A_x}{A_y}\frac{\cos\lambda y}{\sin\lambda y} u_{yB} \quad (7)$$

The driving principle of the MDOF piezoelectric actuator is based on the movement of midpoint P, which is generated by the vibration of the SPPE. Therefore, this study used analysis software to investigate the behavior of the SPPE and to design the MDOF piezoelectric actuator. In the simulation, The PZT material properties of d31, electromechanical coupling coefficient, quality factor, and density were 171 pm/V, 0.34, 1800, and 7.75 g/cm3, respectively. The fixed points of the SPPE were designed on the oscillation nodes to prevent the vibration mode from reducing the driving efficiency of the MDOF piezoelectric actuator. The simulation results demonstrate that the fixed nodes could be located in two zones of the long side of the SPPE, at 3.5–4.5 mm and 11.5–12.5 mm.

A driving voltage was applied to electrodes A and B to verify the trajectory of the micro-pusher. Generating different vibration modes of the SPPE produced three different trajectory directions of the micro-pusher. Figure 2 shows the dynamic SPPE behavior of the micro-pusher under a certain driving voltage and different vibration mode. Figure 2 (I) shows the vibration mode (5V, 5V) as (1,1), in which both electrodes A and B are excited. When the driving voltage is in the peak position (V=Vmax), the micro-pusher of the SPPE exhibits an extension movement in which the micro-pusher moves in a straight line and achieves maximum displacement in the Y direction. When the driving voltage is in the trough position (V=-Vmax), the micro-pusher of the SPPE exhibits a contracting movement. In Figure 2 (II) and (III), when the driving voltage is at position (V= 0V), the micro-pusher of the SPPE is steady. The motion points can be obtained from the excitation electrode toward the floating electrode (Figure 2 (II) and (III)). Therefore, this study employs two parallel symmetric piezoelectric pusher elements (SPPEs) to design and fabricate the MDOF piezoelectric actuator.

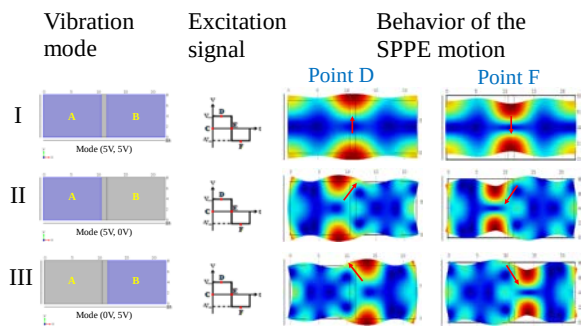

Fig. 2 The dynamic SPPE behavior of the micro-pusher under a certain driving voltage and different vibration mode.

Design of the piezoelectric microactuator

The prototype of the MDOF piezoelectric microactuator is shown in Figure 3, and includes a

hemisphere *device with 160 g weight*, four pairs of SPPEs, conductive springs. To construct the MDOF motion platform, the micro-pushers were placed at the midpoint P of each SPPE by surface mount technology, and the four pairs of SPPEs were arranged on each side of a square grid on the substrate. The micro-pushers were fabricated from Ni alloy using additive manufacturing, an additional advantage of using this material being that the vibration energy generated by the SPPE can efficiently be transmitted to the micro-pushers, enhancing drive efficiency.

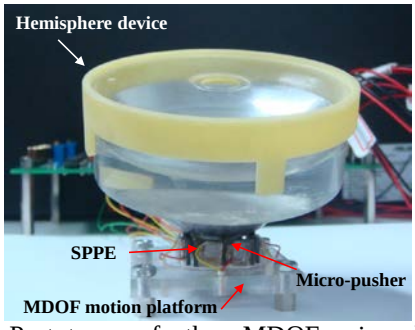

Fig. 3 Prototype of the MDOF piezoelectric microactuator

The driving principle of the MDOF motion platform is mainly the conversion of vibration energy by the micro-pusher into thrust force, which drives the hemisphere *device* to rotate. Three types of vibration modes in combination with different arrangements of SPPEs were used to generate thrust force, making the hemisphere *device* rotate along the X-, Y-, and Z-axes. Figure 4 demonstrates how the MDOF motion platform enables the hemisphere *device* to rotate along the X-, Y-, and Z-axes. Figure 4(a) illustrates that in order to drive the hemisphere *device* to rotate clockwise along the X-axis, a negative voltage signal (V=-Vi) needs to be applied on electrodes A and B of SPPE (I) with vibration mode (1,1) to cause its micro-pusher to move in the (-)Z-direction by contraction movement; at the same time, a positive voltage signal (V=Vi) must be applied on electrodes A and B of SPPE (J) with vibration mode (1,1) to cause its micro-pusher to move in the (+)Z-direction by extension movement; a positive voltage signal (V=Vi) must be applied on electrode A of SPPE (K) with vibration mode (1,0) to cause its micro-pusher to move in the (+)Y- and Z-directions by extension movement; and finally a positive voltage signal (V=Vi) needs to be applied on electrode B of SPPE (L) with vibration mode (0,1) to cause its micro-pusher to move in the (+)Y- and Z-directions by extension movement. Therefore, combining the four individual movements generated by each SPPE, the hemisphere *device* can be driven to rotate in the direction of the X-axis. Figure 4(b) illustrates that to drive the hemisphere *device* to move clockwise along the Y-axis, a positive voltage signal (V=Vi) needs to be applied on electrode B of SPPE (I) with vibration mode (0,1) to cause its micro-pusher to move in the (-)X- and (+)Z-directions by extension movement; at the same time, a positive voltage signal (V=Vi) must be applied on electrode A of SPPE (J) with vibration mode (1,0) to cause its micro-pusher to move in the (-)X- and (+)Z-directions by extension movement; a negative voltage signal (V=-Vi) also needs to be applied on electrodes A and B of SPPE (K) with vibration mode (1,1) to cause its micro-pusher to move in the (-)Z-direction by contraction movement; and a positive voltage signal (V=Vi) must be applied on electrodes A and B of SPPE (L) with vibration mode (1,1) to cause its micro-pusher to move in the (+)Z-direction by extension movement. This combination of the four individual movements generated by each SPPE causes the hemisphere *device* rotor to be driven to move clockwise along the Y-axis. Finally, Figure 4(c) illustrates that to drive the hemisphere *device* rotor to move clockwise along the Z-axis, a positive voltage signal (V=Vi) needs to be applied on electrode A of SPPEs (I), (J), (K) and (L) with vibration mode (1,0) to cause the micro-pushers to move in the (+)X- and Z-directions (I), the (-)X- and (+)Z-directions (J), the (+)Y- and Z-directions (K), and the (-)X- and (+)Z-directions (L), respectively. Thus, combining the four individual movements generated by each SPPE, the hemisphere *device* rotor can be driven to move clockwise along the Z-axis.

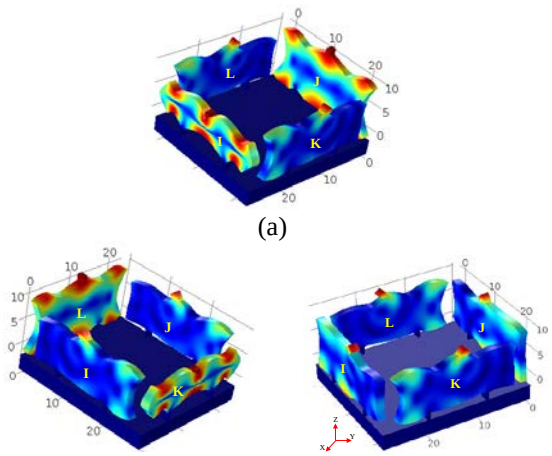

Fig. 4 Rotation along (a) the X-axis; (b) the Y-axis; and (c) the Z-axis.

MEASUREMENT AND EXPERIMENT

The characteristics of MDOF motion platform, including the relationships between rotation speed and driving voltage, were investigated. Table 1 shows the Relation of driving voltage and rotation speed of MDOF motion platform. The driving frequency of the hemisphere device in the X-, Y-, and Z-directions of clockwise rotation were 223.6, 223.2, and 225 kHz, with rotation speeds of 76, 71, and 192 rpm, respectively, at a driving voltage of 30Vpp as shown in Figure 5. When the driving frequency reached the

resonant frequency of each axis, the driving voltage was proportional to the rotation speed. When the drive voltage was 50 Vpp, the rotation speeds along the X-, Y-, and Z-axis were 114, 117, and 332 rpm, respectively as shown Table 1 and Fig. 5. These results indicate that the rotation speeds along the X- and Y-axes are significantly lower than those along the Z-axis. Thus, rotation in the direction of the Z-axis is more efficient. This is because rotation of the hemisphere device along the Z-axis is easier for the micro-pusher to achieve in the direction of inclination; however, for rotation of the hemisphere device along the X- and Z-axis, the micro-pushers must be pushed in the vertical and oblique directions, and the weight of the hemisphere device must be overcome. The difference in speed between the X and Y-axis movements is primarily due to differences in each SPPE caused by the polarization process, which in turn leads to differing thrust between the hemisphere device and the micro-pusher.

Table 1 Relation of driving voltage and rotation speed of MDOF motion platform

Driving voltage (V)	10	30	50
Z-axis (rpm) (@225 kHz)	67	192	332
Y-axis (rpm) (@223.2 kHz)	42	76	117
X-axis (rpm) (@223.6 kHz)	40	74	114

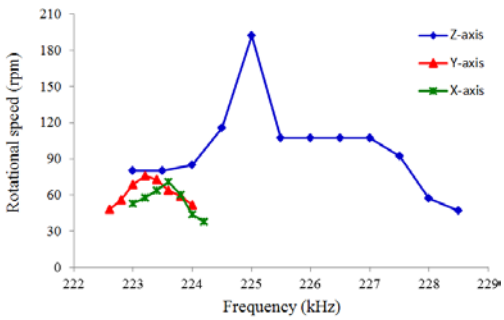

Fig. 5 Relation of driving frequency and rotation speed of MDOF motion platform.

Fig. 6 shows the measured rotating accuracy of the MDOF motion platform. The experiment in this study demonstrated that the the hemisphere device is driven by different modes and rotates around the X-, Y-, and Z-axes. When applying 3 Vpp, and the duty cycle of the drive signal is 5 ms on a MDOF motion platform, the rotating accuracies of the hemisphere device were 0.022°, 0.022°, and 0.007°, and the driving frequencies along the X-, Y-, and Z-axes were 223.6, 223.2, and 225 kHz, respectively. Therefore, the hemisphere device can rotate slowly as shown in Figure 7.

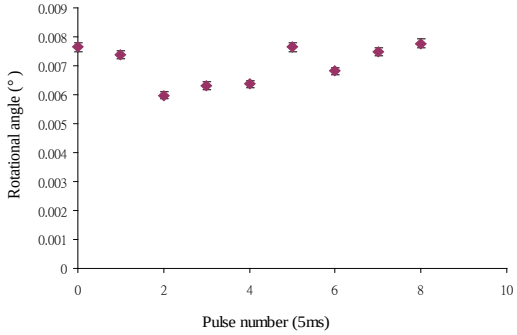

(a) X and Y rotating accuracy of the hemisphere device.

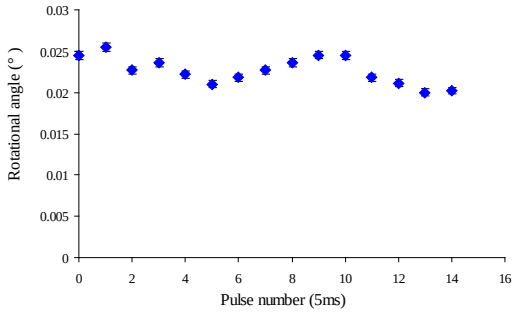

(b) Z rotating accuracy of the hemisphere device.

Fig. 6 The measured rotating accuracy of the hemisphere device.

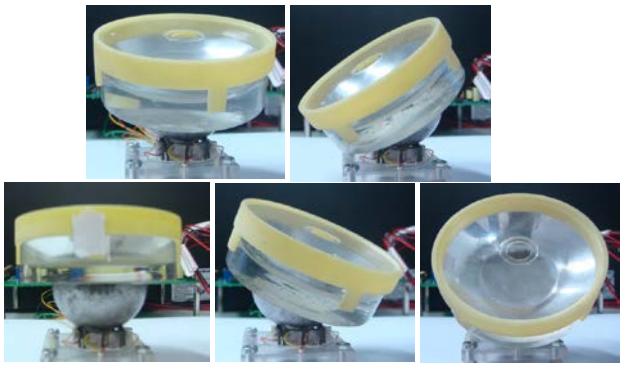

Fig. 7 The hemisphere *device* can rotate slowly under different degrees of rotation.

CONCLUSION

In this study, a piezoelectric microactuator was developed using symmetric piezoelectric plates and Ni alloy micro-pusher elements. An innovative Ni alloy micro-pusher was fabricated using additive manufacturing technology and subsequently attached at the midpoint P of the long side of a piezoelectric plate in order to construct a SPPE. The research integrated AM technology and three different vibration modes were designed in order to develop a MDOF motion platform. The characteristics of MDOF motion platform were measured, and the driving frequencies for rotation of a hemisphere device of 350

g along the X-, Y-, and Z-axes were found to be 223.6, 223.2, and 225 kHz, respectively, while the clockwise rotation speed of the hemisphere device along the X-, Y-, and Z-axes reached 74 rpm, 76 rpm, and 192 rpm, respectively, at a driving voltage of 30Vpp. In summary, a piezoelectric microactuator was successfully developed in this study. In the future, this MDOF motion platform may be used for a number of applications, such as sun-tracking systems for green energy harvesters.

Acknowledgment

The authors would like to thank Ministry of Science and Technology (MOST) and Fisheries Agency for their financial supports to the project (granted number: MOST 103-2221-E-006 -220 -MY3 and 106AS-18.1.7-FA-F1).

REFERENCES

C. Lu, T. Xie, T. Zhou, and Y. Chen, "Study of a new type linear ultrasonic motor with double-driving feet," Ultrasonic, Vol.44, pp. e585-e589, (2006)

K. Otokawa, T. Maeno, "Development of an arrayed-type multi-degree-of-freedom ultrasonic motor based on a selection of reciprocating vibration modes," IEEE Ultrasonic Symposium, vol.2, pp. 1181-1184, (2004)

K. Otokawa, K. Takemura, and T.Maeno, "A multi degree-of-freedom ultrasonic motor using single- phase-driven vibrators," Transactions of the Japan Society of Mechanical Engineers-part C, vol.73, pp. 577-582, (2007)

K. Takemura and T. Maeno, "Design and control of an ultrasonic motor capable of generating multi-DOF motion," IEEE/ASME Transactions on mechatronics, vol.6, pp. 499-506, (2001)

K. Takemura, Y. Ohno and T. Maeno, "Design of a plate type multi-DOF ultrasonic motor and its driving characteristics," in Proceeding IEEE International Conference of Advanced Intelligent Mechatronics, vol.9, pp. 474-480, (2004)

K. Uchino, "Piezoelectric actuators 2006 expansion from IT/robotics to ecological/energy applications, Journal of electroceram," vol. 20, pp. 301-311 (2008)

M. Zhang, W. Guo, and L. Sun, "A multi degree of freedom ultrasonic motor using in-plane deformation of planar piezoelectric elements," Sensors and Actuators A, vol. 148, pp. 193-200, (2008)

Nanomotion LTD., "Ceramic motor," US Patent 5, 453, 653, (1995)

O. Vyshnevskyy, S. Kovalev, and W. Wischnewskiy, "A novel, single-mode piezoceramic plate actuator for ultrasonic linear motors," IEEE Transactions on Ultrasonic, Ferroelectrics and Frequency Control, vol. 52, pp. 2047-2053, (2005)

S. Baglio, S. Castorina, and N. Savalli, "Scaling issues and design of MEMS," New York: Wiley, pp. 124-163 (2008)

S. Toyama, S. Hatae, and M. Nonaka, "Development of multi-degree of feedom spherical ultrasonic motor," in Proceeding IEEE International conference of Advanced Robotics Pisa, Italy, 1, pp. 55-60 (1991)

S. T. HO, "Characteristics of the linear ultrasonic motor using an elliptical shape stator," Japanese Journal of Applied Physics, vol.45, pp. 6011-6013, (2006)

以積層技術實現多軸度壓電致動平台

陳易呈 沈聖智
國立成功大學系統及船舶機電工程學系

陳易呈
工業技術研究院/智慧微系統科技中心/智慧感測機電整合技術部

摘要

本文整合對稱型壓電元件及鎳合金微型推子元件開發多軸度(MDOF)壓電致動平台。其中鎳合金微型推子係利用積層製造(AM)技術研製而成，將其連接在具有雙電極之壓電致動器長邊的中點實現對稱型壓電致動器(SPA)。此微型推子可減少致動器傳遞至轉子的能量損失並增加與轉子間的摩擦力，藉以提高轉動的效率。本研究透過三種不同的 SPA 振動模式，開發出一 MDOF 運動平台，該平台可沿著 X、Y、Z 軸旋轉半球型轉子。實驗結果顯示，MDOF 運動平台沿 X，Y 和 Z 軸的工作頻率分別為 223.6、223.2 及 225 kHz，旋轉速度分別達到 76 rpm、71 rpm 和 192 rpm，驅動電壓則為 30 Vpp。不同於傳統驅動裝置，本研究所設計之 MDOF 運動平台為直驅系統，預期未來可將此設計應用於微型或可攜式裝置，如精密機械手臂之驅動鍊或太陽光源追踪系統等。